

01,07,11,13

Peculiarities of transformation of metastable austenite into deformation martensite during laser cladding with cored wire 60Cr7TiAl

© N.V. Gokhfeld¹, M.A. Filippov², Y.S. Korobov^{1,2}, S.K. Estemirova³, S.O. Morozov²

¹ M.N. Mikheev Institute of Metal Physics, Ural Branch, Russian Academy of Sciences, Yekaterinburg, Russia

² Ural Federal University after the first President of Russia B.N. Yeltsin, Yekaterinburg, Russia

³ Institute of Metallurgy of Ural Branch of the Russian Academy of Science, Yekaterinburg, Russia

E-mail: gokhfeld@imp.uran.ru

Received July 8, 2021

Revised July 13, 2021

Accepted July 16, 2021

Fe-Cr-C-T-Al flux-cored wire surfacing was performed by laser, arc and hybrid methods. Laboratory tests have shown that the deposited layers vary greatly in terms of wear resistance. To identify the reasons, studies were carried out using metallographic, X-ray structural and durometric methods. The analysis of the research results showed that the reason is the difference in the cooling rates of the deposited metal in the range of 1100–800 K. This difference leads to the possibility of the formation of a metastable austenitic structure, which, in turn, affects the wear resistance of the deposited layers.

Keywords: cored wire, wear resistance, metallography, X-ray diffraction, microhardness, laser cladding, arc deposition, hybrid deposition.

DOI: 10.21883/PSS.2022.14.54316.02s

1. Introduction

Alloys based on the Fe-Cr-C system in a certain range of cooling rates, in particular, during arc flame spraying, can form a structure of metastable austenite (MSA) [1]. Such a structure maximally corresponds to the principle of a synergistic approach to non-equilibrium systems. The energy dissipation applied to the working surface under external local action is most effectively carried out by a microheterogeneous structure with metastable austenite, which turns into dispersed martensite at the operation. Self-organization of the structure caused by relaxation processes during the formation of martensite as a result of compressive stresses with a high level of strain hardening of the surface layer provide high resistance to contact action on the surface. In the process of external loading, the hardness of such alloys increases due to hardening of the austenitic and martensite base and the formation of deformation martensite [2–6]. These features allow to use materials with MSA effectively in wear-resistant applications in the form of both base metal [7] and coatings obtained by cladding and thermal spraying [8]. MSA is a promising material both in terms of wear resistance and in terms of alloying efficiency [9]. In particular, such materials include Fe-Cr-C-Al-Ti alloys [10]. The effect of specific heat input and subsequent cooling during technological operations on the phase composition and structure of deposited wear-resistant coatings with metastable austenite and their behavior during abrasive wear requires additional study [11]. Welding and re-

lated technologies are widely used as manufacturing operations. Welding processes differ significantly in the level of heat input, for example, in laser welding, the level of heat input is by 2–3 lower than in arc welding [12]. This results in a difference in the properties of the weld metal due to the degree of overheating, the duration of residence in the molten state and the cooling rate [9].

Different phase composition can be obtained depending on the cooling rate in the temperature range of 1100–800 K. So, only diffusion decomposition of austenite occurs with the formation of a ferrite-cementite structure of various degrees of dispersion (pearlite, sorbite, troostite) at low cooling rates in carbon steel. Above the critical cooling rate, pearlite transformation becomes impossible, austenite diffusion decomposition is suppressed, and austenite undergoes only martensitic transformation. However, if the cooling rate is much higher than the critical one, as in the case of laser cladding (self-hardening effect), then the formation of metastable austenite is possible [11].

The aim of the study was to compare the wear resistance, structure and phase composition of coatings obtained by laser, arc and hybrid cladding methods.

2. Materials, study methods and experimental technique

Laser cladding was carried out on a robotic laser unit with a YAG laser (IPG, Russia). Hybrid cladding was

Table 1. Chemical composition of the flux-cored wire (according to the manufacturer's data)

Chemical composition, weight %					
C	Cr	Al	Ti	S	P
0.620	6.500	1.150	1.180	0.020	0.022

carried out on the same robotic laser complex, but with an additionally connected and synchronized MIG arc welding machine (EVOMIG 350, Russia) in the mode of a general molten pool. Arc welding TIG was carried out manually on the Lorch X 350 (Germany) device. Argon with a purity of 99.998% was used as a shielding gas. The chemical composition of the deposited flux-cored wire of the Fe-Cr-C system is shown in Table 1.

The cladding modes were selected in such a way as to provide a homogeneous monolithic coating according to pre-developed technological modes given in Table 2.

The structure was studied on a Pegasus Quanta-200 electron-scan microscope (FEI, the Netherlands) equipped with an Electron Backscattered Diffraction technique (EBSD) to analyze the bulk phase of austenite or martensite. Indexing of samples for EBSD analysis was more than 90%, and noise reduction (extrapolation of zero solutions) was achieved through the use of built-in software. X-ray diffraction and phase analysis was performed using an XRD-7000 diffraction instrument (Shimadzu, Japan). Shooting conditions: radiation — Cu K_{α} , graphitic monochromator, angular range $2\Theta = 30-100^\circ$, shooting type — step-by-step, scanning step 0.04° , time at point — 3 s. The wear resistance tests of the samples were carried out with abrasive wear on a fixed abrasive. Samples with a cross section of the working part 10×10 mm reciprocated along corundum-based abrasive paper 14A32MN481 (GOST 6456-82) at a speed of 125 mm/s and sample displacement in one double stroke 1.2 mm on the total path length 30 m. The load on the samples was 10 kg (impulse load. 1 MPa). To reduce the lapping period, the working surface 10×10 mm was polished to Ra 0.8.

The abrasive wear resistance was assessed by the results of two parallel tests, the results were compared in rela-

tive units

$$\varepsilon = \Delta M_e / \Delta M_0, \quad (1)$$

where ε — relative wear resistance, ΔM_e — mass wear of the reference sample, ΔM_0 — mass wear of the test sample.

Steel U7 with a hardness of 40 units according to Rockwell was taken as a standard. Sample preparation for structure and microhardness analysis was carried out on QATM metallographic equipment (Germany). Microhardness was measured on a PMT-3 device (Lomo, Russia) at a load of 100 g. To assess the ability of the cladded coating to strain strengthening, the ground side surface of the samples with laser cladding was used to make indentations on a Brinell press with a ball with a diameter of 5 mm at a load of 1000 kg. After that, the hardness was measured in the center of the bottom of the holes (indentations) formed from the introduction of spherical indenters on a Brinell press on a Rockwell device with diamond at a standard load of 150 kg. The deviation from the center of the bottom of the indentations was ± 0.5 mm. At the bottom of each indentation, only one Rockwell hardness measurement was carried out.

3. Results and discussion

3.1. Structural studies before wearing test

The microstructure of the laser cladding sample contains austenitic dendrites with elongated axes of the first order with a width of $10-20 \mu\text{m}$ (Fig. 1). Metallographic analysis of the surface layers of laser cladding showed that the structure is similar to that of steel 50Kh18 [13].

The structure of the alloy after arc cladding is a dendritic and cellular structure with boundary precipitates of a network of dispersed, obviously eutectic, carbonitrides and martensite crystals inside equiaxed grains of inhomogeneous sizes with an average diameter of $10-15 \mu\text{m}$, having a martensitic structure (Fig. 2). Plate martensite crystals form a relief in the form of parallel stripes within one austenite grain.

Hybrid cladding has a dendritic and cellular structure with boundary precipitates, similar to arc cladding, with larger grain-cells with an average diameter of $20-100 \mu\text{m}$ and martensite crystals inside the grains, which also form a striped relief in the form of parallel stripes of parallel orientation within one grain (Fig. 3).

Table 2. Cladding modes

Technology	Cladding method	Power (kW)	Speed of feed (m/min)	Thickness of layer (mm)	Additional parameters
Laser	Robotic laser	3.5	2	4.50 ± 0.1	wobbling (1.5 mm, 300 Hz)
Arc	Hand operated TIG	5	2	4 ± 0.1	General molten pool
Hybrid	Laser + MIG	2 + 3	2	6 ± 0.1	General molten pool

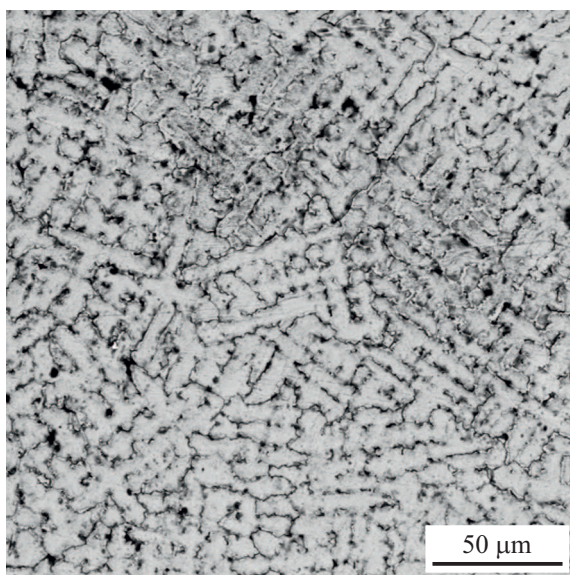


Figure 1. Microstructure of laser cladding in the plane of the cross section.

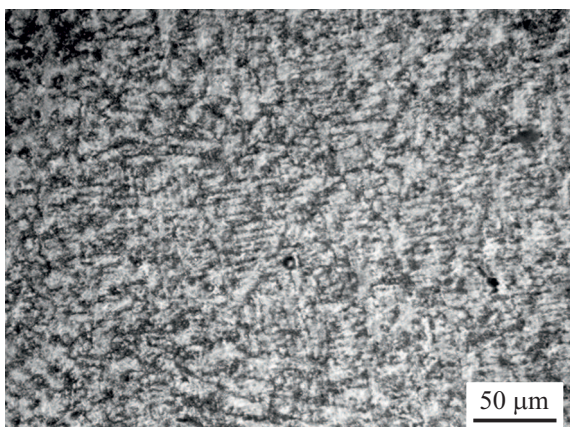


Figure 2. Microstructure of arc cladding in the plane of the cross section.

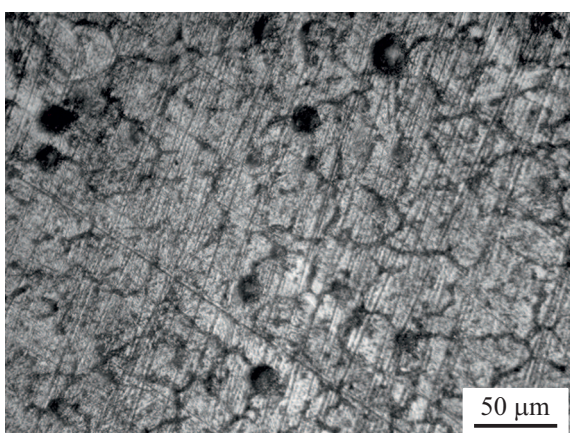


Figure 3. Microstructure of hybrid cladding in the plane of the cross section.

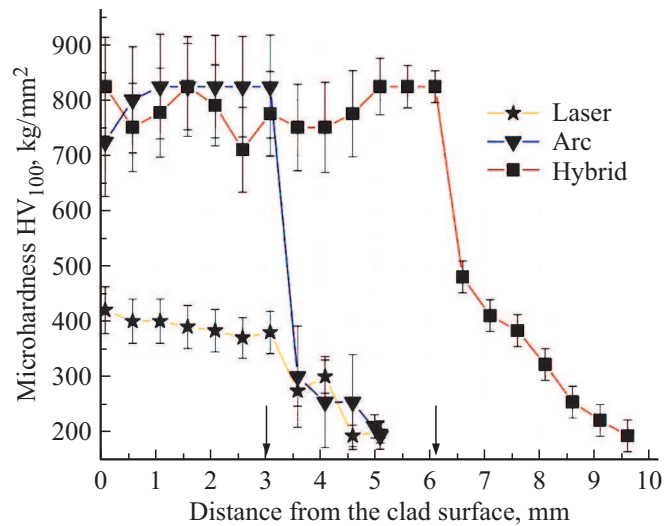


Figure 4. Microhardness of the cladding profile HV_{100} .

3.2. Hardness measurement before wearing test

If in the case of arc and hybrid cladding technology a martensitic structure is formed, then as a result of using a laser for cladding, a structure consisting of metastable austenite [14] is obtained.

It can be seen from Fig. 4 that the hardness of arc and hybrid cladding is much higher than in the case of laser cladding, which is probably due to the difference in structure described above.

3.3. X-ray studies before wearing test

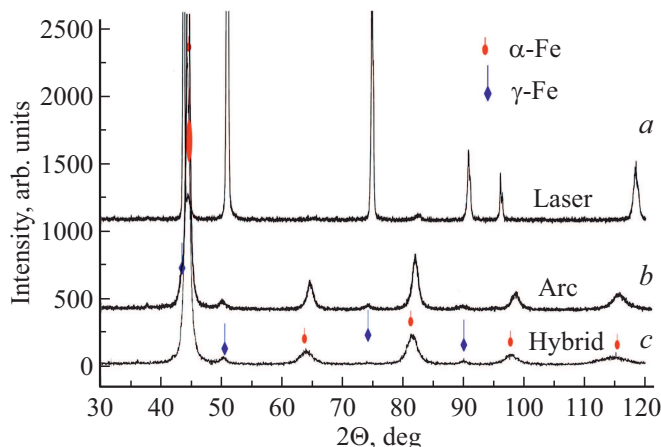
The phase composition and lattice cell parameters for all cladding technologies before wearing tests are given in Table 3.

As can be seen from the X-ray diffraction images (Fig. 5), in the case of arc and hybrid cladding, peak broadening is observed, which indicates that the structure is defective. In case of laser cladding, the peak broadening is minimal.

In Fig. 6, maps of phase distributions on the cross-sectional surface of the studied coatings cladded by various methods are plotted. It can be seen that when using the laser cladding method (Fig. 6, a), approximately 88% of the coating is austenite with a large grain size in the range of 50–150 μm. The sample grain size after arc cladding is smaller (within 1–50 μm), the phase is over 84% martensite (Fig. 6, b). As previously discussed, due to the high heat input in hybrid cladding and arc cladding technology above, a phase transition to martensite occurs, which confirms the EBSD analysis (Fig. 6, b, c) as well as the presence of a large amount of the austenite phase during laser cladding (Fig. 6, a). The phase distribution maps also confirm the results of X-ray analysis (see Fig. 5).

Table 3. Phase composition and lattice cell parameters before wearing tests

Sample	Phase content	Parameters of a lattice cell	
		a , Å	V , Å ³
Laser	$\gamma\text{-Fe}(Fm-3m)$ (> 98%)	3.5900	46.269
	$\alpha\text{-Fe}(Im-3m)$ (< 2%)	2.8624	23.5
Arc	$\gamma\text{-Fe}(Fm-3m)$ (> 9%)	3.6209	47.473
	$\alpha\text{-Fe}(Im-3m)$ (< 91%)	2.8939	24.236
Hybrid	$\gamma\text{-Fe}(Fm-3m)$ (> 4%)	3.6174	47.334
	$\alpha\text{-Fe}(Im-3m)$ (< 94%)	2.8959	24.285
	Iron Chromium Carbide < 2%		

**Figure 5.** X-ray diffraction images of claddings before wearing tests.

3.4. Studies after wearing tests

The results of tests for abrasive wear of the studied steels are given in Table 4.

The table demonstrates that the ability to harden the working surface of laser cladding, estimated by microhardness after wear, exceeds that after hybrid cladding, which is due to the formation of dispersed deformation martensite crystals under the action of moving abrasive particles. In order to prove the metastable properties of austenite, after the strain-induced phase transition to martensite, Rockwell hardness was measured after deformation at the bottom

of the indentation obtained on a Brinell press from ball indentation, according to the values described in the method (see above). The microstructure under the indentation of the ball is similar to martensite in the form of colonies of parallel plates, 2–5 μm wide (Fig. 7).

Apparently, the wave nature of the arrangement of deformation martensite crystals in the form of parallel plates is due to the formation of alternating peaks of compressive stresses at the front of a moving indenter (or abrasive particles during abrasive wear [15] and tensile stresses after the passage of an indenter (particle) in a given metal microvolume (Fig. 7). Martensite crystals with a large specific volume compared to austenite are formed in those regions of austenite where the peak tensile stresses exceed the critical shear value during martensitic transformation. The formation of deformation martensite crystals is accompanied by a micro-trip effect [14]. Since the microstructure demonstrated in Fig. 7 was obtained from a single grain of austenite during deformation, the arrangement of deformation martensite crystals in regular parallel colonies in different grains can be explained by the action of a uniform stress field with the same orientation of the austenite crystal lattice. Reinforcement of the surface with dispersed martensite crystals, which stimulate the micro-trip effect and relaxation of microstresses at the moment of shear, makes it difficult to penetrate the indenter or abrasive particles, increasing the resistance to indenter penetration or wear.

The hardness inside the indentation increased by 20 HRC from the initial one and amounted to 58 HRC, which closely corresponds in value to that obtained by the hybrid cladding technology (Table 3). The magnitude of this increase in hardness is excessive for work hardening and confirms the presence of a martensitic transformation.

The diffraction pattern also shows reflections of impurity phases (Fig. 8), presumably, one of the peaks (in the 42° area) belongs to the Fe₂C phase, orthorhombic system, space group *Pnnm*.

Table 4. Wearing tests

Sample	ΔM , g	ε	HRC	HV_{50} wear
Laser	0.240	3.17	35	770
Arc	0.190	4.00	60	890
Hybrid	0.260	2.92	52	744

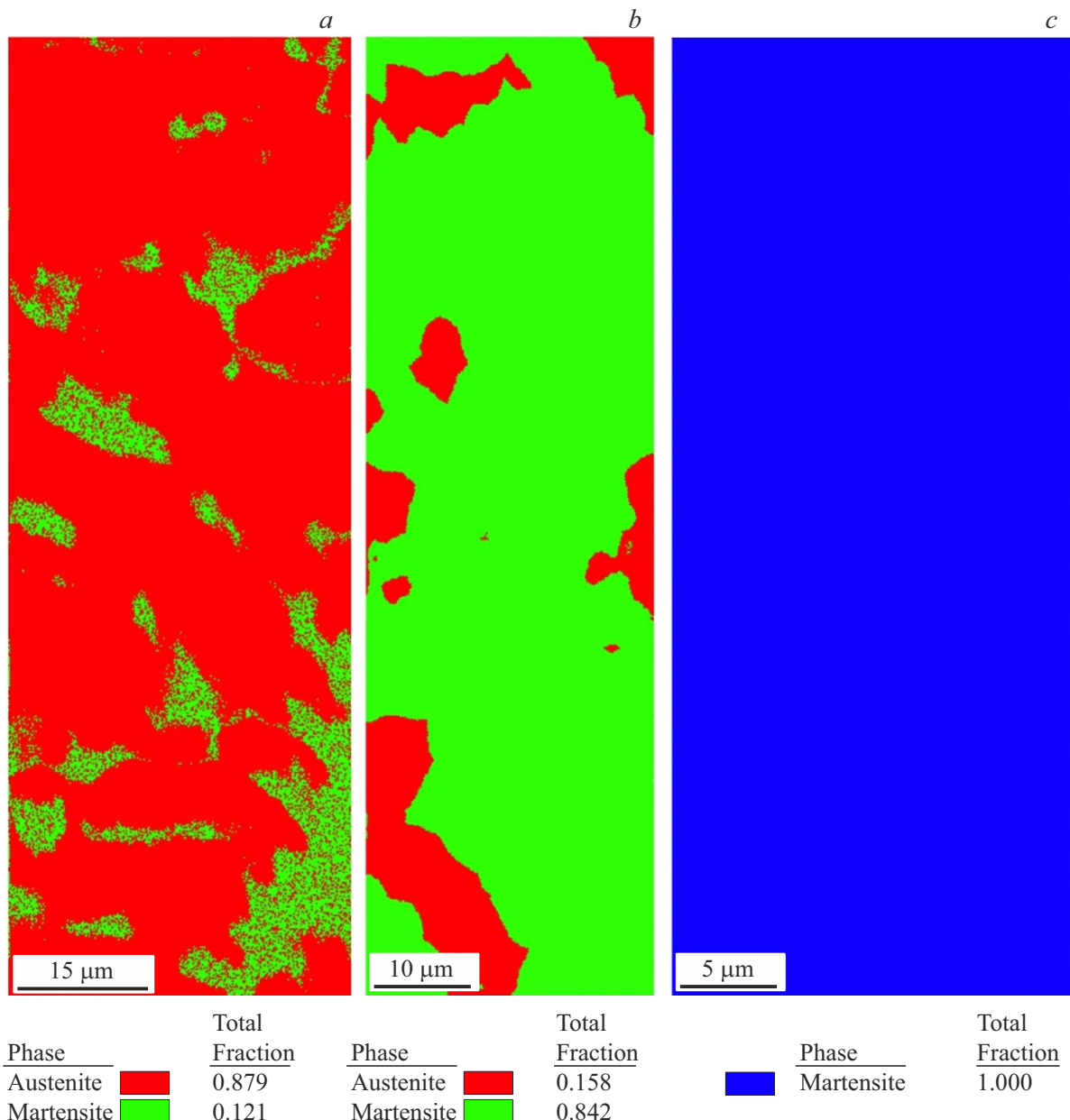


Figure 6. EBSD-map of phase distribution in claddings before wearing tests: a) laser, b) arc, c) hybrid.

Phase composition and lattice cell parameters are shown in Fig. 8 (see the insert). The results of X-ray diffraction analysis also confirm that these numerous stripes represent a cross section of dispersed martensite crystals formed during abrasive wear. The broadening of the peaks, as well as in Fig. 5, confirms the presence of a defective martensitic structure.

4. Conclusion

Based on a comparison of the wear resistance of coatings, it was found that the relative wear resistance for laser cladding is 3.17, which turned out to be even higher than for

hybrid cladding (2.92). It was found that under the action of deformation or wear, metastable austenite transforms into martensite with a hardness corresponding to coatings cladded by arc and hybrid methods.

The high wear resistance of the coating obtained by laser cladding turned out to be higher than that of hybrid cladding, although the hardness of laser cladding is much lower (375 HV_{100}) than that of hybrid (775 HV_{100}) and arc cladding (810 HV_{100}). The wear resistance of laser cladding of the same level with arc cladding is due to the deformation martensitic transformation of metastable austenite. Before loading, the initial hardness of the coating cladded by laser technology was approximately 38 HRC, and

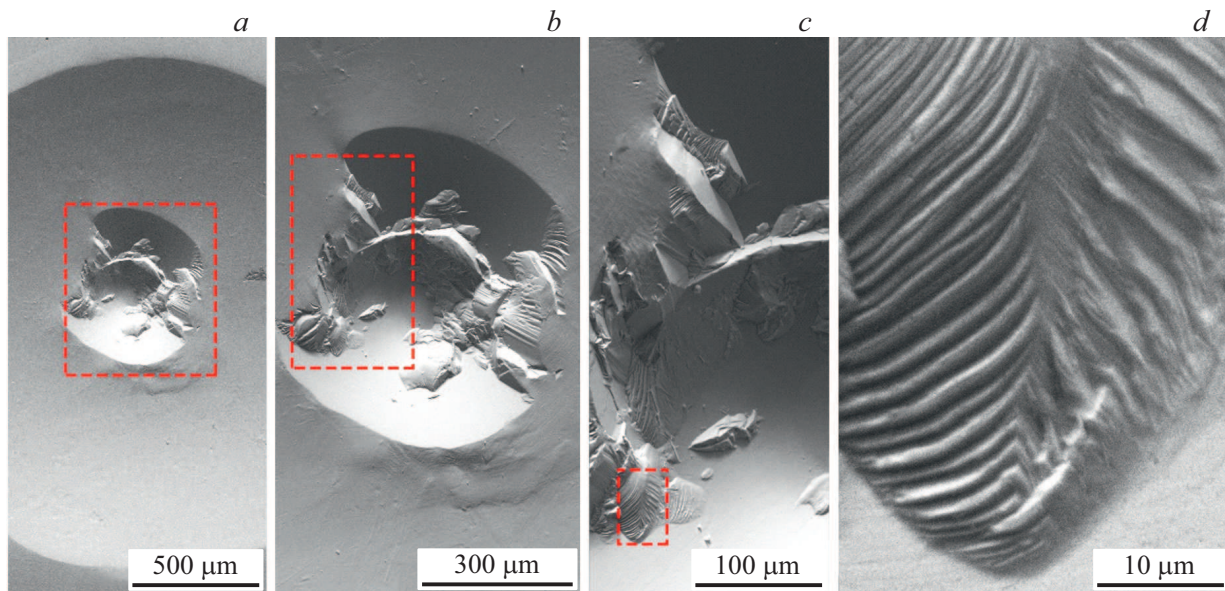


Figure 7. Microstructure inside the ball indentation on laser cladding.

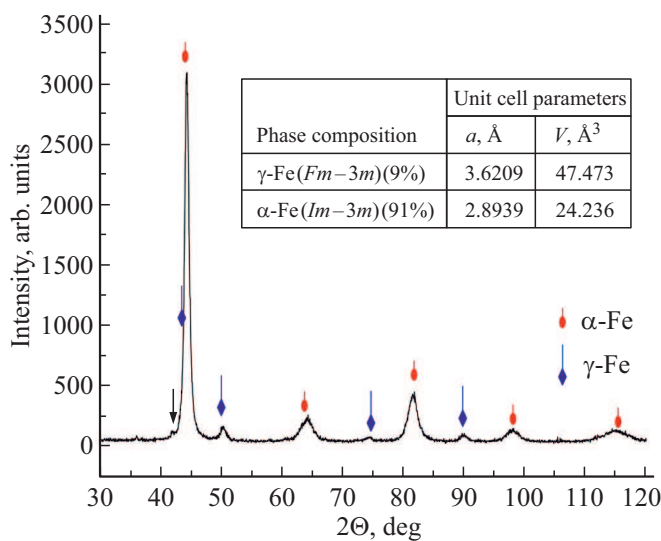


Figure 8. X-ray diffraction images of laser cladding after wearing tests.

after loading it was 58 HRC; thus, the hardness increased by approximately 20 HRC, while the volume of the MSA phase, according to X-ray analysis, before loading was approximately 98%... and only 9% after loading.

Funding

The work was carried out within the framework of the state task of the FASO of Russia for the IPM Ural Branch of the Russian Academy of Sciences on the theme No. AAAA-A19-119070490049-8 and was supported by a grant from the Innovation Promotion Foundation (project IRA-SME No. 58674).

Conflict of interest

The authors declare that they have no conflict of interest.

References

- [1] Y. Korobov, M. Filippov, A. Makarov, I. Malygina, N. Soboleva, D. Fan-tozzi, M. Andrea, H. Koivuluoto, P. Vuoristo. *Coatings* **8**, 2 (2018).
- [2] G. Olson, M. Cohen. *J. Less Common Met.* **28**, 1, 107 (1972).
- [3] C. Wayman. Martensitic transformations: Electron microscopy and diffraction studies. In: *Diffraction and Imaging Techniques in Material Science / Eds S. Amelinckx, R. Gevers, J. Van Landuyt*. 2nd ed. (1978).
- [4] Z. Shi, W. Shao, L. Rao, T. Hu, X. Xing, Y. Zhou, S. Liu, Q. Yang. *Appl. Surface Sci.* **538**, 148108 (2021).
- [5] S. Atamert, H. Bhadeshia. *Mater. Sci. Eng. A* **130**, 1, 101 (1990).
- [6] Y. Korobov, V. Verkhorubov, S. Nevezhin, M. Filippov, A. Tkachuk, A. Makarov, I. Zabolotskikh. An influence of strain-induced nucleation of martensitic transformation on tribological properties of sprayed and surfaced depositions. *International Thermal Spray Conference and Exposition* **8**, 684 (2016).
- [7] M.A. Filippov, G. Yagudin, V. Legchilo, M. Khadiyev, N. Ozerets, S. Estemirova. The use of metastable austenite to increase the wear resistance of steels of the pearlite class. In: *Materials Engineering and Technologies for Production and Processing IV. V. 284 of Solid State Phenomena*, Trans Tech Publications Ltd. (2018).
- [8] A. Pukasiewicz, H. de Boer, G. Sucharski, R. Vaz, L. Procopiak. *Surface Coatings Technology* **327** (2017).
- [9] I. Korobov, O. Pimenova, M. Filippov, M. Khadiev, N. Ozerets, S. Mikhailov, S. Morozov, I. Davydov, N. Razikov. *Procedia Structural Integrity* **14**, 34 (2019).

- [10] Yu.S. Korobov, V.I. Shumyakov, V.E. Prokhorovich, and others. Patent №2692145 C1 Russian Federation, IPC B23K 35/30, C22C 38/28. Wire for welding intermediate-carbon medium alloy armor steels: №2017144969. Applic. 20.12.2017. Publ. 21.06.2019. Applicant Ural Federal University.
- [11] G. Fargas, J. Roa, A. Mateo. Wear **364–365**, 40 (2016).
- [12] J. Zhou, H. Tsai. In: Processes and Mechanisms of Welding Residual Stress and Distortion, Woodhead Publishing Series in Welding and Other Joining Technologies / Ed. Z. Feng. Woodhead Publishing (2005).
- [13] G.R. Desale, C. Paul, B. Gandhi, S. Jain. Wear **266**, 9 (2009).
- [14] M.L. Bernstein, V.A. Zaimovsky, L.M. Kaputkina. Thermomechanical processing of steels. Metallurgiya, M. (1983). 231 p.
- [15] S.M. Nikiforova, M.A. Filippov, A.S. Zhilin. Solid State Phenomena **265**, 10 (2017).